Author(s): Adamson, Jasper; Roithmeyer, Helena; Uudsemaa, Merle; Trummal, Aleksander; Brük, Mari-Liis; Krämer, Sebastian; Reile, Indrek; Rjabovs, Vitalijs; Palmi, Kirsti; Rammo, Matt; Aav, Riina; Kalenius, Elina

Title: Large Azobenzene Macrocycles : Formation and Detection by NMR and MS Methods

Year: 2023

Version: Published version

Please cite the original version:

Adamson, J., Roithmeyer, H., Uudsemaa, M., Trummal, A., Brük, M.-L., Krämer, S., Reile, I., Rjabovs, V., Palmi, K., Rammo, M., Aav, R., & Kalenius, E. (2023). Large Azobenzene Macrocycles : Formation and Detection by NMR and MS Methods. Supramolecular Chemistry, Early online. https://doi.org/10.1080/10610278.2023.2230334

Supramolecular Chemistry

ISSN: (Print) (Online) Journal homepage: https://www.tandfonline.com/loi/gsch20

Large Azobenzene Macrocycles: Formation and Detection by NMR and MS Methods

Jasper Adamson, Helena Roithmeyer, Merle Uudsemaa, Aleksander Trummal, Mari-Liis Brük, Sebastian Krämer, Indrek Reile, Vitalijs Rjabovs, Kirsti Palmi, Matt Rammo, Riina Aav & Elina Kalenius

To cite this article: Jasper Adamson, Helena Roithmeyer, Merle Uudsemaa, Aleksander Trummal, Mari-Liis Brük, Sebastian Krämer, Indrek Reile, Vitalijs Rjabovs, Kirsti Palmi, Matt Rammo, Riina Aav & Elina Kalenius (2023): Large Azobenzene Macrocycles: Formation and Detection by NMR and MS Methods, Supramolecular Chemistry, DOI: 10.1080/10610278.2023.2230334

To link to this article: https://doi.org/10.1080/10610278.2023.2230334

SUPRAMOLECULAR CHEMISTRY
https://doi.org/10.1080/10610278.2023.2230334

Taylor & Francis
Taylor & Francis Group

Large Azobenzene Macrocycles: Formation and Detection by NMR and MS Methods

Jasper Adamson[a], Helena Roithmeyer[a], Merle Uudsemaa[a], Aleksander Trummal[a], Mari-Liis Brük[a], Sebastian Krämer, Indrek Reile[a], Vitalijs Rjabovs[a], Kirsti Palmi[a], Matt Rammo[a], Riina Aav[b] and Elina Kalenius[c]

[a]Laboratory of Chemical Physics, National Institute of Chemical Physics and Biophysics, Tallinn, Estonia; [b]Department of Chemistry and Biotechnology, Tallinn University of Technology, Tallinn, Estonia; [c]Department of Chemistry, NanoScience Center, University of Jyväskylä, Jyväskylä, Finland

ABSTRACT

Azobenzene macrocycles are widely investigated as potential drug delivery systems and as part of molecular machines due to their photo-responsive properties. Herein, we detect the formation of a series of new azobenzene macrocycles that feature up to eight switchable repeating units. High-resolution mass spectrometry and ion mobility (IM) mass spectrometry experiments and ^{1}H and diffusion-ordered spectroscopy (DOSY) NMR are used to detect the presence of the macrocycles that contain 10 to 40 aromatic rings in the gas phase and solution, respectively. The responsiveness of the *Z*-to-*E* photo-switching of the smallest of the macrocycles, exhibiting 2 azobenzene units and in total 10 aromatic rings, separated with column chromatography, is studied with irradiation experiments, using both UV-Vis light and thermal excitation and relaxation, and monitoring the sample with UV-Vis absorption and ^{1}H NMR spectroscopy. DFT calculations are used to understand the conformation of this isolated species in solution.

ARTICLE HISTORY
Received 10 May 2023
Accepted 21 June 2023

KEYWORDS
Large Azobenzene-Containing Macrocycles; Responsive molecules; Photoisomerization; ESI-MS and IM detection

Introduction

Responsive macrocycles, in which a change on the molecular level is brought about by the macrocycle's response to an external stimulus [1–3], are a cornerstone for many applications. In this way, macrocycles that can adjust their conformation and geometry in response to light, temperature, pH or other external stimuli, is used as components of photo-switches [4–6] and parts of molecular machines [7–11]; they can find applicability in catalysis [12,13], smart polymers [14,15], molecular containers [16–18], sensors and other materials to capture specific molecules [19–23]. Moreover, macrocyclic structures that are able to adjust their conformation and thereby guest-binding properties in different biological environments, have the potential to be used as selective and targeted drug delivery and discovery systems [24–27].

Within the field of responsive molecules, azobenzene-containing macrocycles in particular have attracted attention in supramolecular chemistry due to their compliance with the aforementioned criteria. The binding of the guest to these macrocycles can be influenced by changing the physical or chemical environment of the complex, for example, by irradiation with UV-Vis light, as well as by variations in pH, temperature or redox potential [28,29]. Moreover, the molecular movement of a looped molecule around the azobenzene functionalities can be triggered, and the macrocycles can serve as part of molecular machines [30]. The *trans*-to-*cis* photo-switching of several azobenzene-containing macrocycles has been studied for these potential applications and properties. Despite the growing interest in these systems, the currently synthesised azobenzene-containing macrocycles exhibit small sizes with up to 2–8 aromatic units and 1–4 azobenzene moieties [31–33]. The larger size of the azobenzene-containing macrocycles could make it feasible to incorporate sterically more demanding guest molecules and increase the inter- and intramolecular distances within the molecule, which could make the macrocycles attractive for more advanced molecular wires [34,35] or molecular machines [36]. Large macrocycles have been featured for their unique properties in recent years. In 2019, giant calixarenes with up to 90 phenolic subunits were reported as organic nanocompounds

CONTACT Dr. Jasper Adamson jasper.adamson@kbfi.ee Laboratory of Chemical Physics, National Institute of Chemical Physics and Biophysics, Akadeemia tee 23, Tallinn 12618, Estoniae; Dr. Helena Roithmeyer helena.roithmeyer@kbfi.eeDepartment of Chemistry, University of Zurich, Winterthurerstrasse 190, Zurich CH-8057, Switzerland

Supplemental data for this article can be accessed online at https://doi.org/10.1080/10610278.2023.2230334

[37]. Nevertheless, the synthesis of large macrocycles is demanding due to the requirement of sophisticated synthetic strategies to precisely organise monomers in the reaction and suppress oligomeric chain building [38]. In the last year, new studies for azobenzene-containing macrocycles have been published [39,40]. Herein, we present to the best of our knowledge, the first formation and detection of photo-responsive azobenzene macrocycles with up to 40 aromatic rings and eight azobenzene repeating units in a mixture of products. Even though the main products in all performed reactions are consisting of 2 and 4 repeating units and 10 and 20 aromatic rings, respectively, larger macrocycles could be detected with ESI-MS. Commonly synthesised macrocycles often involve expensive or toxic catalysts [41,42]. We tried to avoid these in our reactions and used only Cs_2CO_3 as the sole catalyst. Furthermore, we study the reversible photo-switchable properties of the smallest of these macrocycles. The possibility of isolating the macrocycles in the future with larger yields could provide great interest for their utilisation in the design of responsive nanomaterials. This paper serves as a preliminary study that discusses the formation of these macrocycles with Cs_2CO_3 as the sole catalyst and suggests that such azobenzene-containing structures can form under the conditions studied.

Results and discussion

The target macrocycles in this article are a series of new azobenzene-bearing macrocycles (Scheme 1). For their formation, different reaction methods were attempted to study the influence of the concentration of the reactants, reaction time, base equivalents and temperature on the size of the formed macrocycles in THF. The formed products were detected by ESI-MS in the product mixtures and are described in Table 1. The complete list of experiments is brought in the SI.

Analysis and ESI-MS detection

Five different reaction methods were used to characterise product formation as the reactants were added slowly or instantaneously (Figure S3). In method **A**, all reagents were added simultaneously, while in methods **B** and **C**, a dropwise addition of one reactant for 1 h (**B**) or both reactants for 20 min (**C**) are investigated. In methods **D** and **E**, the influence of temperature on the product formation is investigated by refluxing the reaction mixtures **A** and **C** in THF at 80°C. The equivalents of mild base Cs_2CO_3 are further varied in different reactions.

ESI-MS coupled with ion mobility (IM) studies and NMR spectroscopy were used to analyse the formation of the differently sized macrocycles. During our investigations, IM studies enable the assignment of each macrocycle to a single peak in the ESI-MS spectrum, which are characteristic to the sodium and caesium adducts of the macrocycles. We extract the IM-MS arrival time distributions (ATDs) from the ESI-MS spectra for each compound and assign them to the formed products unambiguously based on the molecular weight as well as isotope distribution in the compounds. The ESI-MS signals with the exact m/z values are used to identify the macrocycles. These ESI-MS results do not give a quantitative indication of the formed macrocycles as the ionisation behaviour of the macrocycles strongly influences signal intensity, but they can be used as an indication of whether the macrocycles form or not under these conditions. Figure 1 shows an illustrative analysis

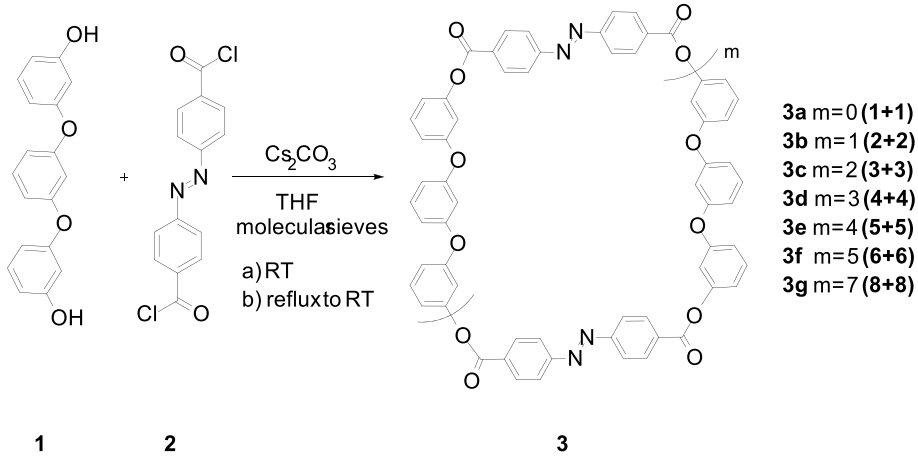

Scheme 1. Route to the macrocycles, containing 1–8 repeating units (m = 0–7), numbers in brackets (1+1 etc.) represent the number of included monomers of 1 and 2.

Table 1. Reaction Conditions and Formed Macrocyclic Products for Reaction Methods A-E.

Entry	Condition	Equiv. Cs_2CO_3	Reaction time (h)	Products ESI-MS
1	A (0, RT)	4	118	**3b,d,e**
2	A (0, RT)	6	144	**3b,d,e,f**
3	B (1, RT)	4	69	**3b,c,d,f**
4	B (1, RT)	6[a]	168	**3b,d**
5	C (2,RT)	4[a]	98	**3b,d**
6	C (2,RT)	6[b]	49	**3b,d**
7	D (0, T)	4[a]	26	**3a,b,d**
8	D (0, T)	6 [a]	29	**3b,d**
9	E (2, T)	4[a]	168	**3b,d**
10	E (2, T)	6[b]	120	**3b,d,e,f,g**

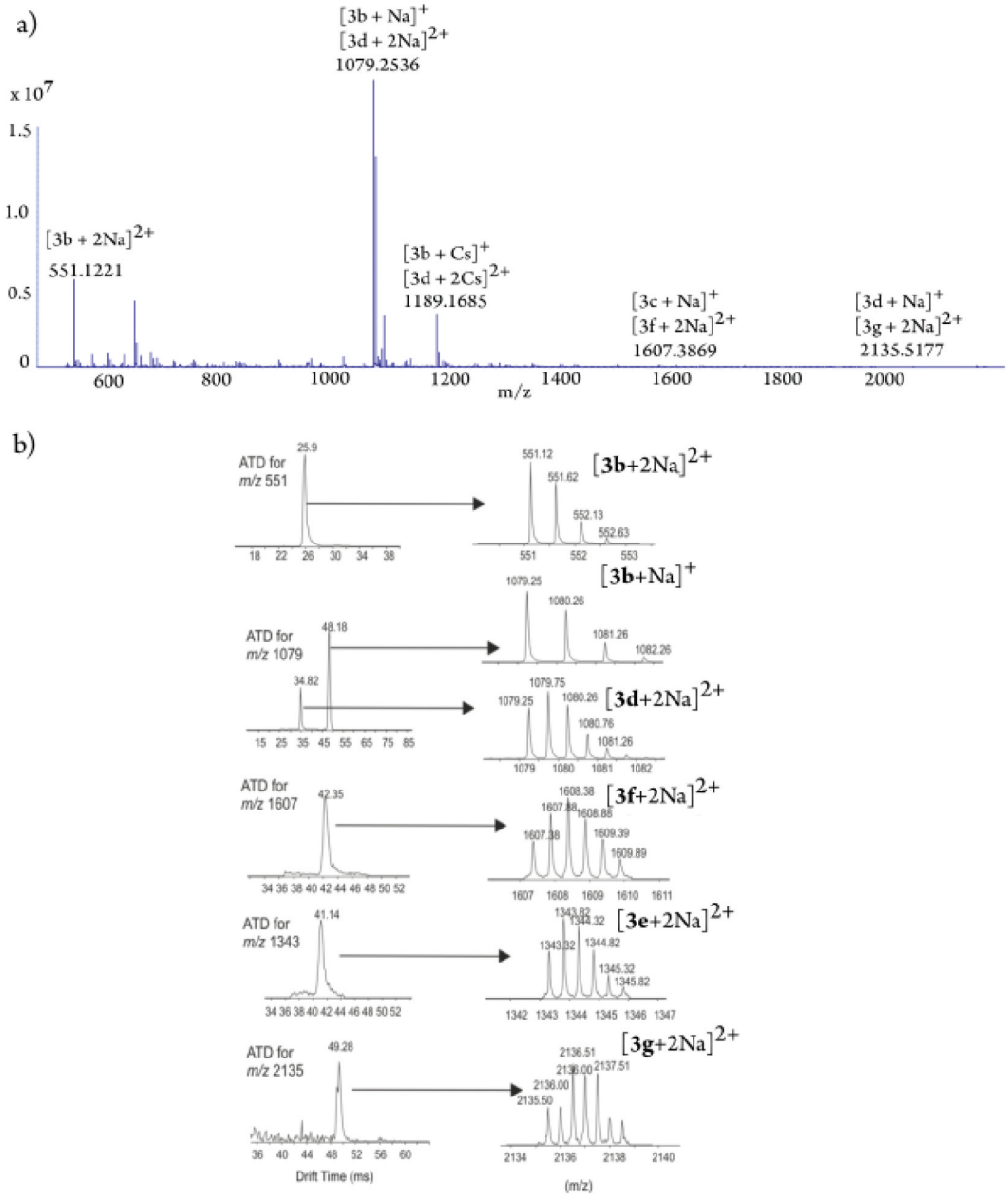

Figure 1. (a) ESI-MS mass spectrum for Table 1, entry 10 and (b) IM-MS arrival time distributions (ATDs) for different ions. Multiple peaks in ATDs correspond to different, overlapping ions. Zoomed views for MS spectra are extracted from each of the peaks to verify their identity and to compare the abundance.

of a product mixture with ESI-MS and IM, where the predominant signals all arise from the formed macrocycles. The other individual ESI-MS spectra and extracted IM signals are brought in the SI for each reaction method. The macrocycles were not isolated in the product mixtures, and we hope that this will be subject to further investigation in the future. The formation of the products in each synthesis method **A-E** is monitored with ^{1}H NMR, and the reactions are quenched after no further changes are seen in the ^{1}H NMR spectra.

Conditions: The dropping time was 1 h, for all reactions. 0 = one pot reaction, 1 = dropping one reactant, 2 = dropping both reactants, RT = stirring at room temperature, $T = 80$°C. [a] Larger amounts of oligomers or side products were observed according to ESI-MS. [b] Purer crude mixtures were obtained from these reactions.

These reaction times are brought in Table 1. DOSY NMR is used to investigate the work-up mixtures of each reaction, however, due to strong deviations in the analysis method, the following reaction evaluation is restricted to the products detected with ESI-MS. The results are indicative that all the synthesis strategies lead to the formation of **3b** (2 + 2) and **3d** (4 + 4) macrocycles. Furthermore, the larger macrocycles **3e – g** form in conditions that use longer reaction times and concentration-controlled conditions. For example, macrocycles **3e** (5 + 5) and **3f** (6 + 6) are formed in reactions **A** and **E** with longer stirring times and 6 equivalents of base, suggesting that a more basic environment and longer reaction times support the formation of larger macrocycles. By virtue of similarity, the giant macrocycle **3 g** (8 + 8) only forms in the concentration-dependent reaction method **E** with 6 equivalents of base with longer stirring times and when applying higher temperature. Macrocycle **3 g** (8 + 8) is only detected as traces in ESI-MS (Table 1, entry 10), which can reflect the weak ionisation behaviour of this large compound or low conversion to this product.

Furthermore, we notice that short reaction times in combination with higher temperature in a one-pot reaction favour the formation of oligomers (method **D**) that are visible based on the broad signals in the ^{1}H NMR spectra, brought in SI. More conversion to the macrocyclic products is obtained in the concentration-dependent methods **C** and **E** with higher base equivalents (Table 1, entries 6 and 10). This is likely to arise from the infinite dilution of one or both of the reactants when added slowly, favouring intramolecular cyclisation kinetics of the formed oligomers. Moreover, higher base equivalents are seen to accelerate the ring-closing step from the oligomers, which is noticeable by the decrease of the broad signals in the ^{1}H NMR spectra when the reactions were monitored over time (Figure S29). It could be possible that the Cs_2CO_3 base may act as a favourable template for the cyclisation of these oligomers [43,44]. We also investigated whether other stoichiometries of the base can have an influence on the macrocycles formed and included reactions with 2 and 8 equivalents of base, but the former conditions of 2 equivalents of base indicate that it is not sufficient for macrocyclization, forming oligomeric species, again evidenced by broad signals in the ^{1}H NMR spectra (Figure S12), while the results from the use of the latter conditions of 8 equivalents of the base are identical to the reactions that used 6 equivalents of the base.

DOSY NMR of the mixtures

We attempted to use DOSY NMR, to relate different diffusion coefficients for the macrocycles in $CDCl_3$ to their molecular weights. An example DOSY NMR spectrum for the mixtures is shown in Figure 2. In general, DOSY NMR can be used to resolve the NMR signals of the components of a mixture according to the components' self-diffusion coefficients that are influenced by their different molecular size, shape and weight.

Large molecules show smaller self-diffusion coefficients and vice versa for small molecules. Nevertheless, different factors, such as molecular interactions, solvents, spectral resolution and even data processing (SI, page S6) can influence and restrict this method's ability to assign specific 1D [1]H peaks to a certain macrocycle. We note that in several instances, it was not possible to differentiate between two macrocyclic compounds with one repeating unit difference in size based on DOSY NMR analysis. We suggest this arises from several factors. Firstly, overlapping signals in the ^{1}H NMR spectra make it difficult to integrate individual signals due to the absence of baseline peak resolution in the direct dimension [45,46].

Furthermore, in the mixtures of the macrocycles, the different molecules with different conformations could interact with each other, thus causing differences in the diffusion coefficients obtained in the DOSY NMR analysis. Moreover, the formed macrocycles can exhibit a non-spherical structure in solution and might even fold due to the multiple switchable functionalities in their structures. Nevertheless, the assignment of the species from DOSY spectra was done based on calibration with respect to three species with known molecular weight. There were deviations in the diffusion constants obtained, which can arise from the macrocycles interaction with each other, the different relative concentrations of macrocyclic homologues or different shapes the macrocycles can adopt. We want to highlight that

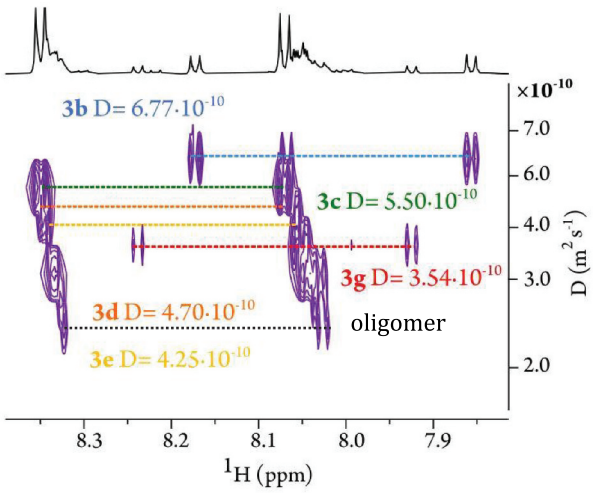

Figure 2. Example DOSY plot from a work-up mixture (obtained from reaction B, Table 1, entry 3) in $CDCl_3$. The peaks in the indirect dimension correspond to different macrocycles with different diffusion coefficients.

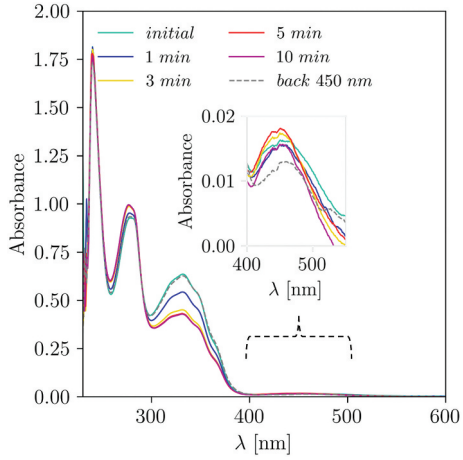

Figure 3. UV-Vis data for the sample of 3b (1.25×10^{-4} M) in CH_2Cl_2, RT, λ = 332 nm. Different irradiation times are marked with different colours.

DOSY NMR is shown for completion and can only be considered in addition to HRMS due to the deviating results from the DOSY analysis. The results from both analysis methods and the relating figures (Mnova) and tables (TopSpin) in the ESI are only indicative assignments.

Responsiveness of the macrocycles

Compound **3b** is separated from the larger macrocycles with column chromatography, details for which is given in the SI with the ESI-MS spectra for the compound in Figure S46.

Both DOSY NMR and MS studies demonstrate that the isolated sample mainly contains the macrocycle **3b**, which could have three possible configurations: ***E,E*-3b**, ***Z,Z*-3b** and ***E,Z*-3b**. We irradiate the isolated sample with UV light at 332 nm for distinct time intervals, followed by an immediate measurement of an UV-Vis absorption spectrum (Figure 3). The *E* to *Z* flip is strongly visible after 10 min of irradiation and a Z-conformer absorption maximum in the 425–450 nm region appeared in the spectra. In addition, a larger peak change in the aromatic region at 275 nm is noticeable, which is often an accompanying change for conversion to the Z-isomer [47–50]. Moreover, the effect of the irradiation could be reversed when irradiated with visible light at 450–500 nm (Figure 3, grey spectrum).

The investigated sample of **3b** exhibits isosbestic points at 290 and 385 nm (Figure 3), which indicates a clean interconversion between two of the macrocycle's isomers. We additionally study this conformational change with ^{1}H NMR spectroscopy (Figure 4). A chemical shift change in different solvents is observed when comparing the ^{1}H NMR spectral chemical shifts in $CDCl_3$ and toluene-d_8. Aromatic-solvent-induced shifts are noticeable in toluene as a solvent, where interactions with the macrocycles π-system can take place by π-stacking or the placement of the molecules in the anisotropic aromatic shielding cone of the solvent aromatic rings [51]. The ^{1}H NMR spectra show characteristic doublets for the azobenzene moieties between 7.5 and 8.5 ppm (Figure 4a, purple spectrum). Moreover, the smaller peaks at 8.1 and 7.8 ppm could indicate that the isolated molecule consists of the ***E,Z***-isomer with a smaller amount of ***Z***-isomer before irradiation. The irradiated ***E,Z*-3b** sample reveals an additional ^{1}H NMR signal in this region at 7.97 ppm. We suggest that this is caused by the transformation of the ***E***-monomer repeat unit of the ***E,Z***-macrocycle to a ***Z***-monomer repeat unit, causing an additional peak rather than increasing the already existing ***Z***-isomer peaks. The exact number of signals in the direct dimension depend on the symmetry of the monomer repeat units and the respective symmetry of the macrocycle. Typically, ***E*** and ***Z*** azobenzenes have only two ^{1}H NMR signals because of mirror planes in the structure. In a macrocyclic architecture, this symmetry can fully or partially be broken, resulting in more than two signals for each monomer repeat unit.

This process is reversible, and we find that irradiation with visible light at 500 nm leads to the relaxation of the macrocycle to the initial state (Figure 4a, yellow spectrum). Similarly, this relaxation is visible with higher temperatures, where the doublet at 7.97 ppm is no longer visible after heating to 358 K (Figure 4b). It is noticeable that the choice of distinct pH ranges allows conversion

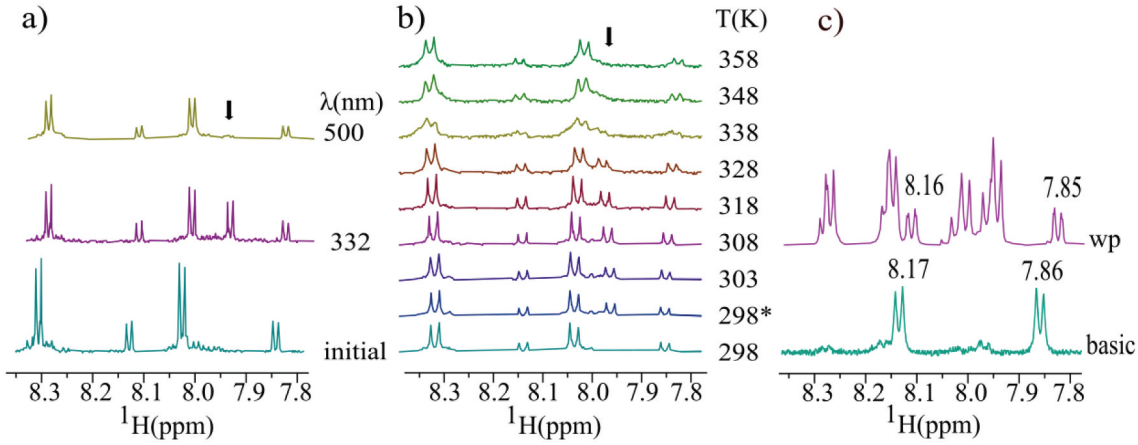

Figure 4. [1]h NMR spectra of irradiation experiments of the sample 3b obtained from reaction B, Table 1, entry 3 and column 2 (SI), in toluene-d8 with a) showing irradiation with 332 nm and 500 nm, each for 40 min; b) variable temperature ^{1}H NMR *after irradiation with *332 nm and c) a product mixture in basic conditions (turquoise spectrum) and after neutralization (wp = work up, purple spectrum, from the sample Table 1, entry 10).

between the configurations of the compounds. Typically, a basic environment favours the ***Z*** configuration of azobenzene [52–55]. We find that when neutralising the basic reaction mixtures, that are obtained from the reactions, the two main peaks at 8.17 and 8.86 ppm decrease and are split into multiple signals during the work-up for the reactions, showing the pH-dependent nature for the *E* and *Z* configurations and thereby the conformations of the products (Figure 4c).

DFT calculations

We performed full geometry optimisations leading to the structures characterised as true minima on the potential energy surface (PES) for the macrocyclic species of ***E,E*-3b** and ***Z,Z*-3b** configurations of **3b** that contain two azobenzene units by carrying out DFT calculations in an implicit chloroform solvent (Figure 5). Furthermore, we performed theoretical

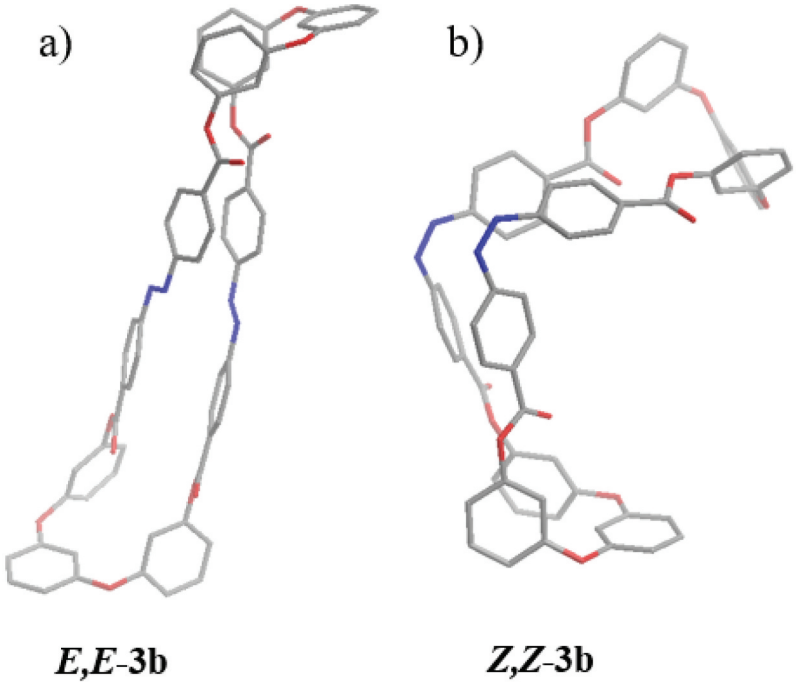

Figure 5. DFT-optimized models for a) E,E-3b and b) Z,Z-3b.

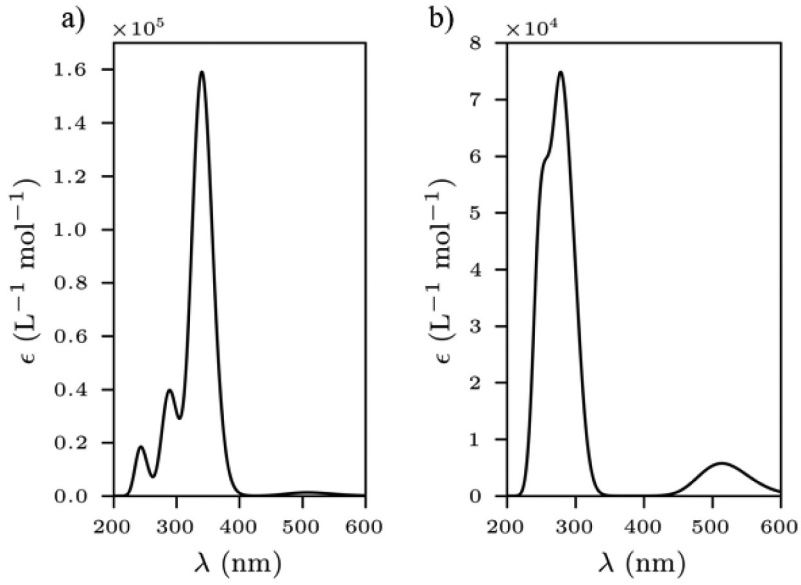

Figure 6. Calculated UV-Vis spectra for a) E,E-3b and b) Z,Z-3b.

calculations of the UV-Vis absorption spectra in chloroform (Figure 6) for both macrocycles.

The representative low-energy structures exhibit different cavity volumes, based on interatomic distances, of 482 Å [3] and 301 Å [3] (Figure S50) and therefore, can suggest potential for size-selective guest binding. It has been reported that the *E*-isomer absorption maximum for the azobenzene molecules lies in the range of 320–360 nm, whereas the largest absorption for the *Z*-isomer is usually located between 400 and 500 nm [56–59]. The UV-Vis spectra for the sample **3b** in Figure 4 contains both of these features.

Conclusion

We demonstrate that the formation of azobenzene containing macrocycles of different ring sizes can be performed with 4 equivalents of Cs_2CO_3 base. The investigated reaction methods **A-E** lead to the main products **3b** and **3d** while higher temperature, reaction time and base equivalents favoured the formation of larger macrocycles **3e-g**. The formation of the macrocycles from oligomers is affected by adjusting the concentration of the reactants and the equivalents of Cs_2CO_3. The macrocycle **3b** is separated from the larger macrocycles, and its response to UV and visible light and temperature is investigated by UV-Vis and ^{1}H NMR spectroscopy. We can see conversion between the configurations of the macrocycle under the influence of UV and visible light and with variable temperature ^{1}H NMR. The UV-Vis spectra from DFT calculations suggest that the isolated species contains both the *E* and *Z* azobenzene configuration. We suggest that arising from the scope of application possibilities of responsive macrocycles, the development of the synthesis of the macrocycles **3a-g** could be of great interest for applications in supramolecular systems.

Supporting Information

Supplementary data (NMR spectra, analysis and ESI-MS /IM analysis examples and theoretical calculations) can be found in the supporting information

Methods

1D ^{1}H and ^{13}C NMR: All spectra were acquired on a 500 MHz Agilent DD2 spectrometer equipped with a 5 mm inverse probe or on an 800 MHz Bruker Avance III spectrometer equipped with a He-cooled 5 mm cryoprobe. All spectra were referenced according to residual solvent signals.

2D DOSY NMR: Diffusion coefficients were referenced to external standards of known molecular weights. Diffusion coefficients were obtained with data analysis by Bruker Topspin T1/T2 module. Further information on DOSY is given in the supporting information.

Mass spectrometry: The mass spectra were measured using Agilent 6560 IM-TOF mass spectrometer connected to dualESI ion source and an ion mobility drift-tube (DT-IM). Samples were diluted in DCM and NaOAc and CsOAc, were used to enhance the ionisation of the macrocycles. Samples were introduced to ion source using direct infusion. Data was acquired using Mass Hunter B.09.00 software and analysed with Mass

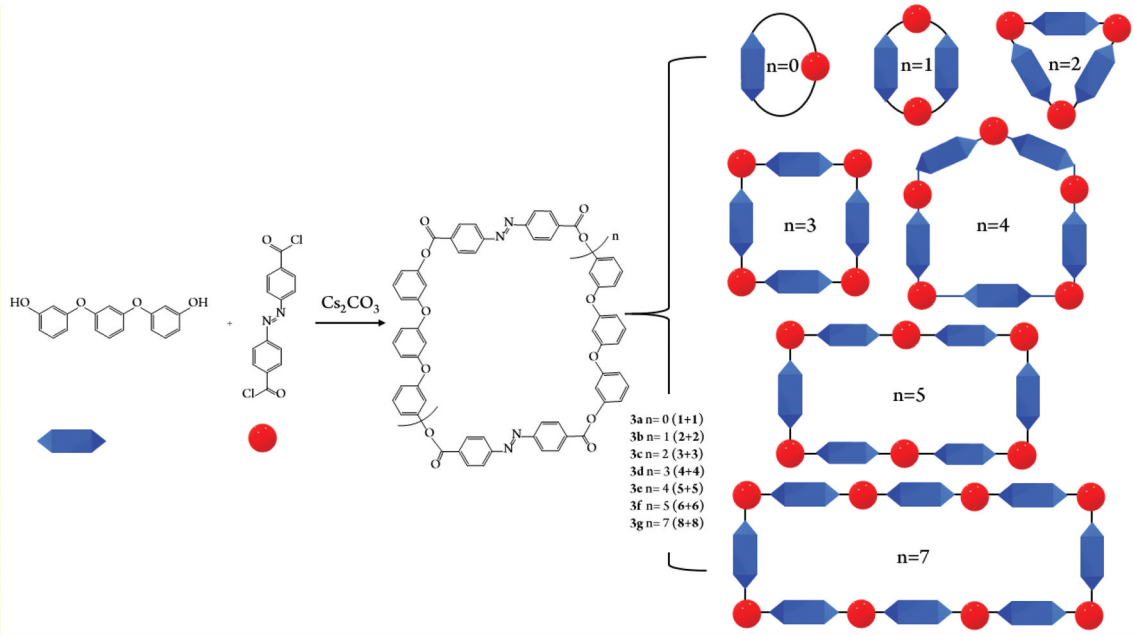

Synthesis and detection of large macrocycles with up to 8 responsive azobenzene and 40 aromatic units. The isomerisation of the products can be controlled with external stimuli such as light, pH and temperature. The structures were detected with ESI-MS and IM and NMR methods.

Hunter Qualitative Analysis B.07.00 and IM-MS Browser B.08.00. For more detailed information see SI.

UV-Vis spectroscopy: The measurements were conducted on a SHIMADZU UV-3600 Plus Spectrophotometer equipped with three different detectors: PMT, InGaAs and PbS.

Irradiation source: For the irradiation experiments, a femtosecond laser system from Light Conversion was used, comprising the pump laser (Pharos-SP), optical parametric amplifier (Orpheus-HE), and second harmonic generator (Lyra-SH) with average output intensities of 200 mW and 70 mW for 332 nm and 500 nm wavelengths, respectively. The samples were irradiated for 1, 3, 5, 10 and 20 min. or 40 min. and measured with UV/Vis in between. Irradiation wavelengths were set to 332 nm, 450 nm or 500 nm.

Acknowledgments

The authors gratefully acknowledge financial support by the Ministry of Education and Research, Republic of Estonia (grants PSG400, PRG661 and PRG399), the Estonian Center of Analytical Chemistry (TT4), the European Regional Development Fund (project TK134 "EQUITANT") and instrumentation of the University of Jyväskylä.

Disclosure statement

No potential conflict of interest was reported by the author(s).

Author contributions

HR designed and planned the synthesis of the macrocycles, performed the synthesis, NMR and MS measurements and analysed the data gathered from all experiments. MU and AT carried out quantum chemical calculations. MLB did preliminary synthesis work. SK developed a software program for automatic ESI-MS peak analysis. IR and VR helped with the DOSY NMR investigation. KP helped with NMR irradiation experiments. MR prepared the irradiation source. RA supervised the work of MB on preliminary synthesis. EK supervised and planned all ESI-MS and IM measurements at the University of Jyväskylä and helped to analyse the data. JA conceived, coordinated and supervised the project. HR and JA wrote the paper with input from all authors.

References

[1] Geng W-C, Sun H, Guo D-S. Macrocycles containing azo groups: recognition, assembly and application. J Incl Phenom Macrocyclic Chem. **2018**;92(1–2):1–79. doi: 10.1007/s10847-018-0819-8

[2] Gilissen PJ, White PB, Berrocal JA, et al. Molecular motor-functionalized porphyrin macrocycles. Nat Commun. **2020**;11(1):1. doi: 10.1038/s41467-020-19123-y

[3] Mishra KA; Adamson J; Öeren M; Kaabel S; Fomitšenko M; Aav R. Dynamic Chiral Cyclohexanohemicucurbit[12]Uril. Chem Comm. **2020**;56(93):14645–14648. doi: 10.1039/D0CC06817A

[4] Heindl AH, Becker J, Wegner HA. Selective switching of multiple azobenzenes. Chem Sci. **2019**;10(31):7418–7425. doi: 10.1039/C9SC02347J

[5] Li Z, Liang J, Xue W, et al. Switchable Azo-Macrocycles: from Molecules to Functionalisation. Supramol Chem. **2014**;26(1):54–65. doi: 10.1080/10610278.2013.822970
[6] Eleya N; Ghosh S; Lork E; Staubitz A. A new photo switchable azobenzene macrocycle without thermal relaxation at ambient temperature. J Mater Chem C Mater. **2021**; 9 (1):82–87. doi: 10.1039/D0TC05211F
[7] Balzani V, Credi A, Raymo FM, et al. Artificial molecular machines. Angew Chem. **2000**;39(19):3348–3391. doi: 10.1002/1521-3773(20001002)39:19<3348:AID-ANIE3348>3.0.CO;2-X
[8] Ariga K. The evolution of molecular machines through interfacial nanoarchitectonics: from toys to tools. Chem Sci. **2020**;11(39):10594–10604. doi: 10.1039/D0SC03164J
[9] Sauvage J-P. From chemical topology to molecular machines (nobel lecture). Angewandte Chemie. **2017**;56(37):11080–11093. doi: 10.1002/anie.201702992
[10] Murakami H; Kawabuchi A; Matsumoto R; Ido T; Nakashima N. A multi-mode-driven molecular shuttle: photochemically and thermally reactive azobenzene roTaxanes. J Am Chem Soc. **2005**;127(45):15891–15899. doi: 10.1021/ja053690l
[11] Wang W-K; Xu Z-Y; Zhang Y-C; Wang H; Zhang D-W; Liu Y; Li Z-T. A tristable [2]rotaxane that is doubly gated by foldamer and azobenzene kinetic barriers. Chem Comm. **2016**;52(47):7490–7493. doi: 10.1039/C6CC02110G
[12] De Rosa M; La Manna P; Soriente A; Gaeta C; Talotta C; Neri P. Exploiting the hydrophobicity of calixarene macrocycles for catalysis under "on-water" conditions. RSC Adv. **2016**;6(94):91846–91851. doi: 10.1039/C6RA19270J
[13] Santos E, Carvalho C, Terzi C, et al. Recent advances in catalyzed sequential reactions and the potential use of tetrapyrrolic macrocycles as catalysts. Molecules. **2018**;23(11). doi: 10.3390/molecules23112796
[14] Qi Z, Schalley CA. Exploring macrocycles in functional supramolecular gels: from stimuli responsiveness to systems chemistry. Acc Chem Res. **2014**;47(7):2222–2233. doi: 10.1021/ar500193z
[15] Sun Y, Wang Z, Li Y, et al. Photoresponsive amphiphilic macrocycles containing main-chain azobenzene polymers. Macromol Rapid Commun. **2015**;36 (14):1341–1347. doi: 10.1002/marc.201500136
[16] Jordan JH, Gibb BC. Molecular containers assembled through the hydrophobic effect. Chem Soc Rev. **2015**;44(2). doi: 10.1039/C4CS00191E
[17] Kobayashi K, Yamanaka M. Self-assembled capsules based on tetrafunctionalized calix[4]resorcinarene cavitands. Chem Soc Rev. **2015**;44(2). doi: 10.1039/C4CS00153B
[18] Ballester P, Fujita M, Rebek J. Molecular Containers. Chem Soc Rev. **2015**;44(2). doi: 10.1039/C4CS90101K
[19] Sinn S, Biedermann F. Chemical sensors based on cucurbit[*n*]uril macrocycles. ISR J Chem. **2018**;58(3–4):357–412. doi: 10.1002/ijch.201700118
[20] Chen Z, Wang Q, Wu X, et al. Optical chirality sensing using macrocycles, synthetic and supramolecular oligomers/polymers, and nanoparticle based sensors. Chem Soc Rev. **2015**;44(13):4249–4263. doi: 10.1039/C4CS00531G
[21] Wong J, Todd M, Rutledge P. Recent advances in macrocyclic fluorescent probes for ion sensing. Molecules. **2017**;22:2. doi: 10.3390/molecules22020200
[22] Liu Y; Wang H; Shangguan L; Liu P; Shi B; Hong X; Huang F. Selective separation of phenanthrene from aromatic isomer mixtures by a water-soluble azobenzene-based macrocycle. J Am Chem Soc. **2021**;143(8):3081–3085. doi: 10.1021/jacs.1c01204
[23] Wang L; Tu Y; Valkonen A; Rissanen K; Jiang W. Selective recognition of phenazine by 2,6-dibutoxylnaphthalene-based tetralactam macrocycle. Chin J Chem. **2019**;37 (9):892–896. doi: 10.1002/cjoc.201900233
[24] Norouzy A, W N. Synthetic macrocyclic receptors as tools in drug delivery and drug discovery. Drg Target Review. **2014**;10:10 .
[25] Moussa YE, Venkataramanan NS, Wheate NJ. Demonstration of the first known 1: 2 host-guest encapsulation of a platinum anticancer complex within a macrocycle. J Incl Phenom Macrocyclic Chem. **2020**;96 (1–2):145–154. doi: 10.1007/s10847-019-00960-4
[26] Moussa YE, Ong YQE, Perry JD, et al. Demonstration of in vitro host-guest complex formation and safety of para-sulfonatocalix[8]arene as a delivery vehicle for two antibiotic drugs. J Pharm Sci. **2018**;107 (12):3105–3111. doi: 10.1016/j.xphs.2018.08.016
[27] Nikolova V, Velinova A, Dobrev S, et al. Host–Guest complexation of cucurbit[7]uril and cucurbit[8]uril with the antineoplastic and multiple sclerosis agent mitoxantrone (novantrone). J Phys Chem A. **2021**;125(2). doi: 10.1021/acs.jpca.0c08544
[28] Yu J, Qi D, Design LJ. Design, synthesis and applications of responsive macrocycles. Commun Chem. **2020**;3 (1):189. doi: 10.1038/s42004-020-00438-2
[29] Pascal S; Lavaud L; Azarias C; Varlot A; Canard G; Giorgi M; Jacquemin D; Siri O. Azacalixquinarenes: from Canonical to (Poly-)Zwitterionic Macrocycles. J Org Chem. **2019**;84(3):1387–1397. doi: 10.1021/acs.joc.8b02847
[30] Yamamoto T; Nakamura D; Liu G; Nishinaka K; Tsuda A. Synthesis and photoisomerization of an azobenzene-containing tetrapyrrolic macrocycle. J Photochem Photobiol A Chem. **2016**;331:66–75. doi: 10.1016/j.jphotochem.2015.08.006
[31] Liu Y; Wang H; Liu P; Zhu H; Shi B; Hong X; Huang F. Azobenzene-Based macrocyclic arenes: synthesis, crystal structures, and light-controlled molecular encapsulation and release. Angewandte Chemie. **2021**;60 (11):5766–5770. doi: 10.1002/anie.202015597
[32] Sahid Hossain M, Chatterjee S, Bandyopadhyay S. Azobenzene-based photochromic delivery vehicles for ions and small molecules. Chem Eur J. **2022**;28(63). doi: 10.1002/chem.202201902
[33] Ouyang G; Bialas D; Würthner F. Reversible fluorescence modulation through the photoisomerization of an azobenzene-bridged perylene bisimide cyclophane. Org Chem Front. **2021**;8(7):1424–1430. doi: 10.1039/D0QO01635G
[34] Humphrey JL; Lott KM; Wright ME; Kuciauskas D. Second hyperpolarizability of ethynyl-linked azobenzene molecular wires. J Phys Chem B. **2005**; 109(46):21496–21498. doi: 10.1021/jp054980r

[35] Kume S, Kuroiwa K, Kimizuka N. Photoresponsive molecular wires of feii triazole complexes in organic media and light-induced morphological transformations. Chem Comm. **2006**;23:2442. doi: 10.1039/b603477b

[36] Aprahamian I. The Future of Molecular Machines. ACS Cent Sci. **2020**;6(3):347–358. doi: 10.1021/acscentsci.0c00064

[37] Guérineau V; Rollet M; Viel S; Lepoittevin B; Costa L; Saint-Aguet P; Laurent R; Roger P; Gigmes D; Martini C; Huc V. The synthesis and characterization of giant calixarenes. Nat Commun. **2019**; 10(1):113. doi: 10.1038/s41467-018-07751-4

[38] Grave C, Schlüter AD. Shape-persistent, nano-sized macrocycles. European J Org Chem. **2002**; 2002 (18):3075–3098. doi: 10.1002/1099-0690(200209)2002:18<3075:AID-EJOC3075>3.0.CO;2-3

[39] Nieland E, Voss J, Mix A, et al. Photoresponsive dissipative macrocycles using visible-light-switchable azobenzenes. Angewandte Chemie. **2022**;61(48). doi: 10.1002/anie.202212745

[40] Ghosh S, Eschen C, Eleya N, et al. Synthesis of a series of 12-membered azobenzene macrocycles and tuning of the half-life of the thermal *z* – *E* Isomerization. J Org Chem. **2022**;88(6):3372–3377. doi: 10.1021/acs.joc.2c00549

[41] Zhu H; Shangguan L; Shi B; Yu G; Huang F. Recent progress in macrocyclic amphiphiles and macrocyclic host-based supra-amphiphiles. Mater Chem Front. **2018**;2(12):2152–2174. doi: 10.1039/c8qm00314a

[42] Heindl A; Schweighauser L; Logemann C; Wegner H. Azobenzene macrocycles: synthesis of a z-stable azobenzenophane. Synthesis (Stuttg). **2017**; 49 (12):2632–2639. doi: 10.1055/s-0036-1589006

[43] Langton MJ, Xiong Y, Beer PD. Active-metal template synthesis of a halogen-bonding rotaxane for anion recognition. Chem Eur J. **2015**; 21(52):18910–18914. doi: 10.1002/chem.201504236

[44] Bols PS; Anderson HL. Template-directed synthesis of molecular nanorings and cages. Acc Chem Res. **2018**;51(9):2083–2092. doi: 10.1021/acs.accounts.8b00313

[45] Nilsson M; Connell MA; Davis AL; Morris GA. Biexponential fitting of diffusion-ordered nmr data: practicalities and limitations. Anal Chem. **2006**;78 (9):3040–3045. doi: 10.1021/ac060034a

[46] Nilsson M. The DOSy toolbox: a new tool for processing pfg nmr diffusion data. J Magn Reson. **2009**; 200 (2):296–302. doi: 10.1016/j.jmr.2009.07.022

[47] Norikane Y; Hirai Y; Yoshida M. Photoinduced isothermal phase transitions of liquid-crystalline macrocyclic azobenzenes. Chem Commun. **2011**;47(6):1770–1772. doi: 10.1039/C0CC04052E

[48] Rajakumar P; Senthilkumar B; Srinivasan K. Synthesis of azobenzenophanes with a large molecular cavity. Aust J Chem. **2006**;59(1):75. doi: 10.1071/CH05254

[49] Bonvallet PA, Mullen MR, Evans PJ, et al. Improved functionality and control in the isomerization of a calix[4]arene-capped azobenzene. Tetrahedron Lett. **2011**;52 (10):1117–1120. doi: 10.1016/j.tetlet.2010.12.107

[50] Molina-Muriel R; Romero JR; Li Y; Aragay G; Ballester P. The effect of solvent on the binding of anions and ion-pairs with a neutral [2]Rotaxane. Org Biomol Chem. **2021**;19(45):9986–9995. doi: 10.1039/D1OB01845K

[51] Zhu Y; Tang M; Zhang H; Rahman F-U; Ballester P; Rebek J; Hunter CA; Yu Y. Water and the Cation–π Interaction. J Am Chem Soc. **2021**;143 (31):12397–12403. doi: 10.1021/jacs.1c06510

[52] Kortekaas L; Simke J; Arndt NB; Böckmann M; Doltsinis NL; Ravoo BJ. Acid-catalysed liquid-to-solid transitioning of arylazoisoxazole photoswitches. Chem Sci. **2021**;12(34):11338–11346. doi: 10.1039/D1SC03308E

[53] Dunn NJ; Humphries WH; Offenbacher AR; King TL; Gray JA. PH-Dependent cis → trans isomerization rates for azobenzene dyes in aqueous solution. J Phys Chem A. **2009**; 113(47):13144–13151. doi: 10.1021/jp903102u

[54] Fitz J; Mammana A. Spectroscopic study of the ph dependence of the optical properties of a water-soluble molecular photo-switch. Spectrochim Acta A Mol Biomol Spectrosc. **2020**;227:117576. doi: 10.1016/j.saa.2019.117576

[55] Ludwanowski S; Ari M; Parison K; Kalthoum S; Straub P; Pompe N; Weber S; Walter M; Walther A. PH tuning of water-soluble arylazopyrazole photoswitches. Chem Eur J. **2020**;26(58):13203–13212. doi: 10.1002/chem.202000659

[56] Leistner A, Kirchner S, Karcher J, et al. Fluorinated azobenzenes switchable with red light. Chem Eur J. **2021**; 27(31):8094–8099. doi: 10.1002/chem.202005486

[57] Łukasik N; Hemine K; Anusiewicz I; Skurski P; Paluszkiewicz E. Photoresponsive amide-based derivatives of azobenzene-4,4′-dicarboxylic acid—experimental and theoretical studies. Materials. **2021**; 14(14):3995. doi: 10.3390/ma14143995

[58] Samanta D, Gemen J, Chu Z, et al. Reversible photoswitching of encapsulated azobenzenes in water. Proc Nat Acad Sci. **2018**;115(38):9379–9384. doi: 10.1073/pnas.1712787115

[59] Bandara HMD; Burdette SC. Photoisomerization in different classes of azobenzene. Chem Soc Rev. **2012**;41 (5):1809–1825. doi: 10.1039/C1CS15179G